https://doi.org/10.5194/egusphere-2023-2515
Preprint. Discussion started: 15 December 2023

Recent Ice sheet surface warming events over coastal Dronning Maud Land, East Antarctica: Causes and Implications

Eledath M Gayathri[1,2], Chavarukonam M Laluraj[1], Karathazhiyath Satheesan[3], Kenichi Matsuoka[4] and Meloth Thamban[1]

[1]National Centre for Polar & Ocean Research, Ministry of Earth Sciences, Goa, India
[2]School of Earth, Ocean and Atmospheric Sciences, Goa University, Taleigao Plateau Goa, India
[3]Department of Atmospheric Sciences, School of Marine Sciences Cochin, University of Science and Technology, Cochin, Kerala, 682016, India
[4]Norwegian Polar Institute, Tromsø, Norway

Correspondence to: Eledath M Gayathri (gayathriem@ncpor.res.in)

Abstract. Sudden short term warming events over the ice sheet surface (hereafter Ice Sheet Surface Warming (ISSW) events) can affect mass balance by sublimation and on rare occasions melting when the temperature rises above 0 °C. On the one hand, the knowledge of the frequency and duration of these warming events is essential, while on the other hand, a process- level understanding of them is crucial for incorporating in climate models and tracing their behaviour in future climate scenarios. Here, we examined the ISSW events over coastal Dronning Maud Land (cDML) in East Antarctica using borehole temperature record of an ice core covering a period of 2014-18 CE. The borehole surface thermistor record provided accurate estimation of year-round ISST and subsurface heat flux in the region. In total, 71 warming events (> 2 ºC for > 3 days) with a maximum warming of 11 °C were recorded during the period. They mostly occurred during spring (24) and winter (23), followed by autumn (15) and least in summer (9). The general meteorological setting during these events was the occurrence of strong winds. It was found that 84 % of ISSW events occurred during strong easterly winds with high snow accumulation, while 16% occurred during strong southeasterly winds (katabatic) without any precipitation. The study suggests that for the first case, intense downward longwave radiation associated with warm air advection (with moisture from the surrounding ocean) heated the ice sheet's surface and led to snowfall. For the second case, turbulent mixing due to strong and dry winds from the interior of the continent (katabatic) led to ISSW. Furthermore, the synoptic conditions during ISSW events differed by changes in the relative positions of low pressure and high pressure over southern ocean. Considering the drastic drop in accumulation in cDML since 1906 CE, a simultaneous increase in ISSW events (via their sublimation and melting rates), appears to have greater implications on the mass balance and stability of coastal Antarctic ice sheets in the long term.

1. Introduction

Ice Sheet Surface Temperature (ISST) is an integral factor in determining ice sheet's mass balance and stability. It affects the accumulation and ablation of ice sheets through melting and sublimation, especially in the escarpment and

https://doi.org/10.5194/egusphere-2023-2515
Preprint. Discussion started: 15 December 2023

coastal areas where the wind speed changes drastically (M. R. Van Den Broeke, 1997). The atmosphere interacts with the ISST complexly by changing the surface energy balance via changes in net radiation and turbulent heat flux at the surface. Atmospheric warming and increased cloud cover resulted in high downward longwave radiation at the surface, which led to Ice Sheet Surface Warming (ISSW) over Antarctica for the last decades (Sato & Simmonds, 2021). Episodic short-term warming events are projected to increase over Antarctica by the end of this century (Feron et al., 2021). They can cause a sudden rise in ISST and may lead to surface melt over coastal areas for a few days in summer. The ice sheet-atmospheric interaction has regional differences, and the drivers of such ISSW events can vary according the location, elevation, topography and prevailing meteorological conditions.

There are several studies of individual atmospheric warming events over different regions of Antarctica (Scott et al., 2019; Turner et al., 2021; Wille et al., 2019; Zou et al., 2021a, 2021b). Over the pacific sector of West Antarctica, the intrusion of warm, moist air was found to cause a sudden rise in temperature and melting (Emanuelsson et al., 2018; Ghiz et al., 2021; Nicolas and Bromwich, 2011; Nicolas et al., 2017). It happens more often during El Niño events (Nicolas et al., 2017). There are several observations of warming events over the west and east Antarctica due to warm air advection (Sinclair, 1981; Wille et al., 2019; Zou et al., 2021a, b). Similarly, the warming events over the eastern Antarctic Peninsula and Mc Murdo dry valleys in the Transantarctic Mountains has been attributed to the episodic mountain winds called foehn (Bozkurt et al., 2018; Cape et al., 2015; Speirs et al., 2010; King et al., 2017). Such foehn wind events triggered the collapse of the ice shelves of Larsen A in 1995 (Rott et al., 1996) and the Larsen B in 2002 (Scambos et al., 2004) over the Antarctic peninsula (van den Broeke, 2005; Scambos et al., 2000). A warming event over the Amery Ice Shelf in East Antarctica has been reported to be from warm air advection associated with an atmospheric river and high katabatic winds (Turner et al., 2022). On the contrary, persistent katabatic winds have warmed the surface in the Roi Baudouin Ice Shelf in Dronning Maud Land (Lenaerts et al., 2017). The effect of these directionally constant, persistent katabatic winds in surface warming is signified further by the presence of a thermal belt over the coastal Antarctic regions with strong katabatic winds (Kikuchi et al., 1992; King, 1998). The intensity and duration of wind induced warming mainly depend on the synoptic conditions and topography of the region (Bromwich et al., 1993; Heinemann, 2000). Since the evolution of the surface temperature in the Antarctica is complex due to local and large-scale influences, a regional-scale study is proposed for its holistic understanding.

The ISST is not always coherent with changes in air temperature because it is affected by other factors like wind speed, topography and ultimately surface energy balance. Therefore, it is necessary to use insitu temperature measurements over the ice sheets to explain the ice sheet warming events. The present study is the first attempt to identify the short-term events of ISSW using borehole thermal records from the coastal Dronning Maud Land (cDML) region for five years (2014-18 CE). The objective of this study is to identify the drivers of ice surface warming events using daily surface temperature recorded by thermistors installed into a bore hole in cDML.

2. Data and methodology

2.1 Study Region

https://doi.org/10.5194/egusphere-2023-2515
Preprint. Discussion started: 15 December 2023

The study area, coastal Dronning Maud Land (cDML), is situated in the Atlantic sector of the Southern Ocean (Figure 1a). Dronning Maud Land covers a large area of East Antarctica, with its 2000 km long coast characterized by extensive ice shelves interspersed with numerous ice rises and rumples that have a key role in the stability of the ice sheet (Matsuoka et al., 2015; Goel et al., 2020). The interior of this region is partly separated by high mountains, causing steep ice surface slopes from the continental plateau towards the coastal areas. The Nivlisen Ice Shelf downstream of our study site is subject to reasonably small oceanic melting (Lindbäck et al., 2019) and large surface mass balance with a strong east-west gradient (Pratap et al., 2022). The surface mass balance of DML varied spatially due to local orography and surface wind effects (Thiery et al., 2012; Rotschky et al., 2007; Lenaerts et al., 2014). Averaged snow accumulation from an ice core from cDML region provides values in the range of 0.07-0.15 m of water equivalent for the last two decades (Ejaz et al 2021). Ice cores from Eastern DML showed an increase and Western DML a decrease in snow accumulation for the last century (Altnau et al., 2015; Philippe et al., 2016). Such high temporal variability in accumulation over the region is attributed to cyclonic activities along the coastal areas of DML (Schlosser and Oerter, 2002). In addition, these high temporal variabilities in accumulation patterns can also be influenced by moisture transport and atmospheric dynamics (Vaughan et al., 1999; Lenaerts et al., 2013), which affects the transport and deposition of atmospheric aerosols to the surface of ice sheets (Kreutz et al., 2000).

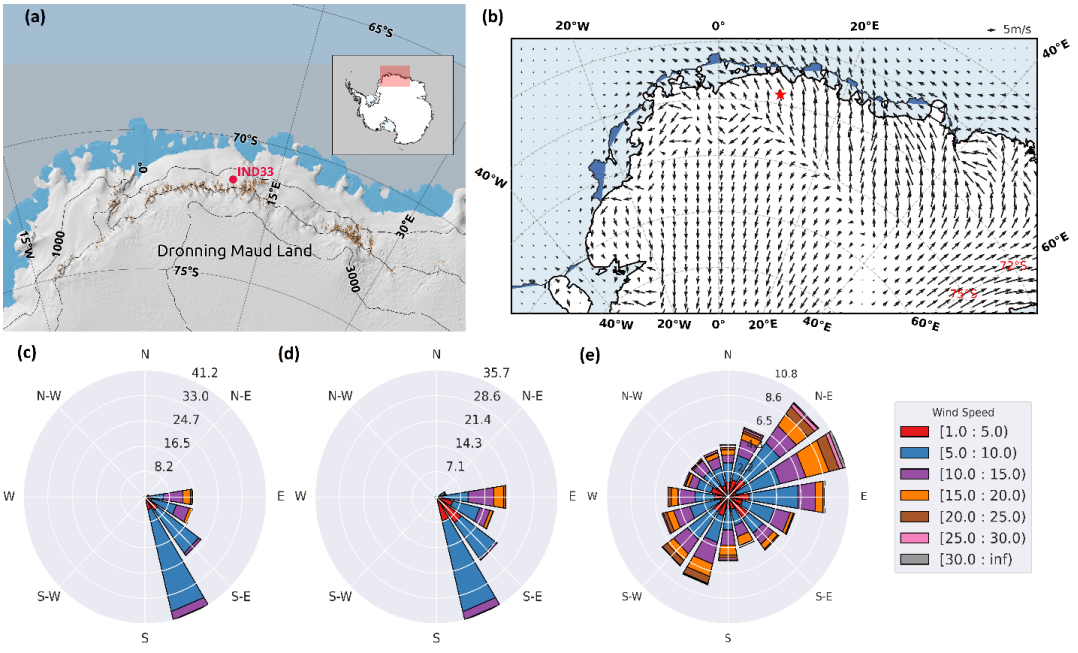

Figure 1: (a) Study region Coastal Dronning Maud Land, with borehole location marked. The region is near to a high mountain range and the surface sloping from interior towards the coast (Lowther et al., 2022). Map of study region made using Quantarctica (Matsuoka et al., 2021) (b) Climatology of surface level wind pattern using zonal and meridional wind components from ERA5 dataset over the continent with borehole location marked as a red star. (c-e) Wind roses for the

https://doi.org/10.5194/egusphere-2023-2515
Preprint. Discussion started: 15 December 2023

period 2014-2018 at the surface, at 850 hPa and at 500 hPa level, respectively. Radial lines give the percentage of occurrence of wind in that particular direction. Color code represents wind speed with magnitude in the insect figure.

The borehole is situated at 1470 m a.s.l. and relatively flat region of ice sheet compared to the rock outcrops nearby, and close to the grounding zone (~10 km inland) with small ice-flow speed (3-4 ma^{-1}). Further inland to the location is east-west oriented Wohlthat Mountains (Hui et al., 2014) ~ 20 km from the borehole location. In our analysis, the average air temperature for the study period was -22 °C from ERA5 reanalysis data, whereas, mean wind speed was about 8 ms^{-1} but largely variable (Figure 1b and c-e). On the surface (10 m), these winds are cold and termed katabatic, since they originate from elevated interior of the continent. Similarly, winds at 850 hPa (~ 1 km above sea level) is predominantly south-easterlies. However, at 500 hPa (~ 5 km above sea level), the wind is disorganized, and blowing from all directions, but preferring north easterly direction. In addition to the above wind structure, there are episodic easterly winds that bring moisture and precipitation to the region. They usually originate from the climatological low present over the southern Atlantic Ocean (centered at 25 °E). The cDML is frequently affected by synoptic intrusions and associated high precipitation events (Noone et al., 1999; Schlosser et al., 2010). Such episodic high precipitation events contribute to the majority of the precipitation in the region and tend to heat the surface to several degrees. (Hirasawa et al., 2000; Massom et al., 2004; Schlosser et al., 2010; Noone et al., 1999; Sinclair, 1981).

2.2 Borehole temperature measurements

A set of thermistor-string assemblies was placed in the borehole after the retrieving an ice core (IND-33/B8) during 2013 CE (core location in Figure 1a). The thermistor set assembly consists of 36 thermistors connected to thermometry strings placed in different levels (six thermistors above the surface up to 1.2 m and 30 thermistors below up to 30 m) and a data logger (RST instruments, Canada). The thermistors were installed at 20 cm intervals from 1 m height to 1 m depth, and then 25 and 50 cm from 1-2 m depth and 2-4 m depth respectively. Below that, they were placed at 1 m interval. The sensors had an accuracy of 0.01 °C and were pre-calibrated. The data logger (of specification DT 2040) was fixed next to the borehole in a 1-m pit and firmly secured to a bamboo stick. The thermistors were placed one day after drilling completion. The sensors started functioning from 5th January 2014 to 15th December 2018, regularly taking measurements in 6-hour intervals. The data was retrieved from the logger thrice, in January 2014, in December 2017 and in December 2018.

2.3 Reanalysis and model data

Since in-situ meteorological observation is unavailable at the borehole site, we used the 5th generation ECMWF reanalysis (ERA5) data. The data gives hourly records of atmospheric parameters at the surface level with a grid resolution of 0.25°x 0.25°. The data obtained for the study are; (1) Surface energy balance parameters - Net shortwave and longwave radiation, total downward longwave radiation, sensible heat flux and latent heat flux; (2) Meteorological conditions- wind speed and wind direction at the surface (10 m) and upper levels (850 hPa, 500 hPa), cloud fraction,

https://doi.org/10.5194/egusphere-2023-2515
Preprint. Discussion started: 15 December 2023

air temperature (2 m) and precipitation; and (3) Synoptic conditions – Mean Sea level pressure, zonal and meridional components of vertically integrated water vapour transport (IVT). Over Antarctica, although the upper level meteorological conditions are represented well in ERA5, the surface level conditions suffer some biases, especially surface temperature and surface energy balance parameters (Silber et al., 2019; Zhu et al., 2021). Hence, we compared the 2 m air temperature with two in situ measurements and energy balance parameters with an AWS observation and RACMO2.3p2 model output (Supplementary Figures 3s, 4s and 5s). ERA5 dataset was qualitatively consistent with in situ and model datasets, even though their magnitudes differed. Since we are looking at the variability and not on the absolute values, the data from ERA5 would be appropriate for this study. The validation of ERA5 dataset is elaborated in the discussion (Section 4.1).

2.4 Calculation of subsurface conductive heat flux and determination of surface energy balance

Surface energy balance is the sum of all the incoming and outgoing energy fluxes; the net heat flux,

$$Q = SWnet + LWnet + SHF + LHF + G \quad (1)$$

Where 'SWnet' is the net shortwave radiation (sum of incoming and outgoing SW radiation), 'LWnet' is the net longwave radiation (sum of incoming and outgoing LW radiation), and SHF is sensible heat flux. All the above fluxes are positive when directed toward the surface. Latent heat flux (LHF) is negative for sublimation and positive for condensation. Subsurface conductive heat flux G is positive when directed towards the surface and negative when directed into the snowpack.

The subsurface conductive heat flux (G) required for the estimation of surface energy balance is calculated from the surface and subsurface temperature measurements, using Fourier's law of heat conduction;

$$G = -Ke\frac{dT}{dz} \quad (2)$$

Where T is the temperature and z is the depth (negative downwards). The heat flux towards the ice pack is negative, whereas towards the surface is positive. The heat flux at all depths up to 10 m (considering that after this level, there is no penetration of heat from above over the period we studied) is calculated and added the individual fluxes to get the net conductive heat flux.

Ke (in W m^{-1} K^{-1}) is the effective thermal conductivity and is estimated as a function of density (ρ in kgm^{-3}) using the equation (Östin and Andersson, 1991).

$$Ke = -0.00871 + 0.439 \times 10^{-3} \times \rho + 1.05 \times 10^{-6} \times \rho^2 \quad (3)$$

https://doi.org/10.5194/egusphere-2023-2515
Preprint. Discussion started: 15 December 2023

Density at each level is directly obtained by measuring the top 10 m ice core sections. Short-wave penetration into the snowpack was neglected for fine-grained, dry Antarctic snow (Brandt and Warren, 1993). The calculated subsurface conductive heat flux is shown in the supplementary information (Supplementary Figure 1s).

The sublimation rate (in m.w.e) of the surface is calculated from latent heat flux (LHF) and latent heat of sublimation, L_s (2.83×10^6 Jkg^{-1}) and ρ_w is density of water.

$$Sublimation\ rate = \frac{LHF}{Ls \times \rho w} \quad (4)$$

3. Results

3.1 Retrieval of ice sheet surface temperature

The thermistors recorded temperatures at different levels from a depth of 30 m to a height of 1.2 m at an interval of 20 cm immediately close to the surface (from the height of 1.2 m to the depth of 1 m). We derived surface temperature from these data. Figure 2a represents the daily average temperature measured at the surface level thermistor from 2014-2018. Over the years, the maximum and minimum temperatures and the magnitude of day-to-day fluctuations of surface level thermistor decreased. This dampening in temperature could be a result of the burial of thermistors each year by the annual snow accumulation. In other words, the surface level thermistor during the deployment no longer records the surface temperature by 2018, rather gets buried by each year's snow accumulation. The buried thermistors record smaller fluctuations than the surface thermistors, and the exposed ones record larger fluctuations. This is evident from the profile of temperature at different levels for summer and winter shown in Fig. 2 (c) and (d)). To consider burial, the average annual accumulation of the time period is determined. Table 1 gives the annual surface mass balance from RACMO2.3p2 and ERA5.

https://doi.org/10.5194/egusphere-2023-2515
Preprint. Discussion started: 15 December 2023

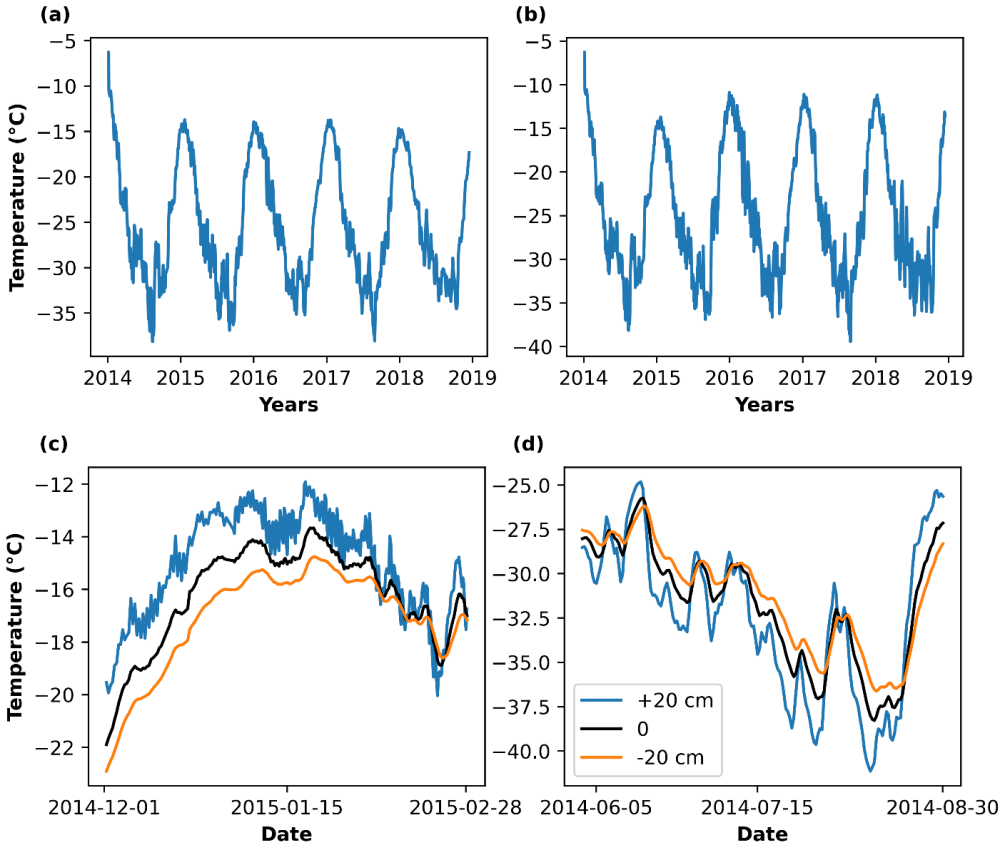

Figure 2: (a) The surface temperature time series from the surface level thermistor without considering burial. (b) The time series of surface temperature after applying burial criteria (c-d) The time series of temperature measured by sensors at the surface level (0) and 20 cm upper (+20 cm) and lower levels (-20 cm) for summer and winter respectively.

Year	Precipitation (cm) from ERA 5	Sublimation (cm) from ERA 5	Accumulation (cm) = Precipitation – Sublimation	Surface mass balance from RACMO (cm)
2014	17.47	6	11	7.2
2015	21.61	7	14	6.5
2016	19.32	7	12	7.3
2017	15.9	5	10	-
2018	19.3	6	13	-

Table 1: Annual accumulation from ERA5 and surface mass balance from RACMO model for 2014-2018. Surface mass balance is the sum of all the accumulation and ablation processes. RACMO data is limited to June 2017 only.

https://doi.org/10.5194/egusphere-2023-2515
Preprint. Discussion started: 15 December 2023

The average annual accumulation (accumulation - sublimation) over the years was ~12 cm estimated from ERA5. This does not include snow drift, hence somewhat overestimating the net accumulation. We examined the surface mass balance by RACMO model run at 5.5 km resolution in DML (van Wessem et al., 2018; Lenaerts et al., 2017). It considered total precipitation, sublimation and snow drift for estimating surface mass balance which showed an average of ~7 cm/year for 2014-2016. This gave an approximate time of burial of surface thermistor which later corrected manually by maintaining uniformity in temperature fluctuations (Noone et al., 1999). Accordingly, we took surface temperature values from the sensor on the surface when installed for January 2014-September 2015, a height of 20 cm for October 2015-December 2017, and finally, 40 cm for 2018. Figure 2b shows the final temperature time series after considering burial. The depths selected may not be accurate due to biases in the precipitation and sublimation data and the large distance between thermistors (20 cm). However, the errors in depths of +/- 20 cm can be permissible since these levels correlate well with the surface (r value between 20 cm above and surface = 0.986 and between 20 cm below and surface =0.987. Both the values have $p < 0.001$). The time series of temperature at the surface level, 20 cm above the surface and 20 cm below the surface for 2014 (Supplementary Figure 2s) shows that all the fluctuations were synchronous at the three levels with different amplitude of fluctuation. There was a horizontal movement of sensors parallel to the region's ice flow (3-4 myr^{-1}). Since it does not affect our study, its horizontal movement with time was ignored.

3.2 Selection of warming events

The warming events were observed as continuous rises in the daily average temperature profile. The onset of an event is defined as when the temperature starts to rise and marks an end when the temperature falls or stabilizes. Figure 3 shows the examples of some warming events and the shaded regions are the duration of the events. The temperature during 5-13 May 2018 stabilized after 13 May, marking the event's end, similar to events during 10-15 July 2016, 11-14 July 2015 and 27 September – 4 October 2017 (Figure 3b,c, g and h). Whereas the rest of the events (Figure 3a, d, e and f) had a decrease in temperature marking the end of the events. The warming of each event was calculated as the difference between the temperatures of the end and start dates and duration, as the number of days between the start and end dates. There were 140 events during the study period with a warming of 0.2 °C to 11 °C. Among the events, ~50 % of the warming was < 2 °C. Hence, to incorporate the top 50 % of warming events, we constrained the selection of events to warming greater than 2 °C. These events had a duration greater than or equal to 3 days. Thus, applying this selection criterion, the number of events reduced to 71 for 2014-2018. These events were examined for their mechanism of warming and synoptic conditions favoring it.

https://doi.org/10.5194/egusphere-2023-2515
Preprint. Discussion started: 15 December 2023

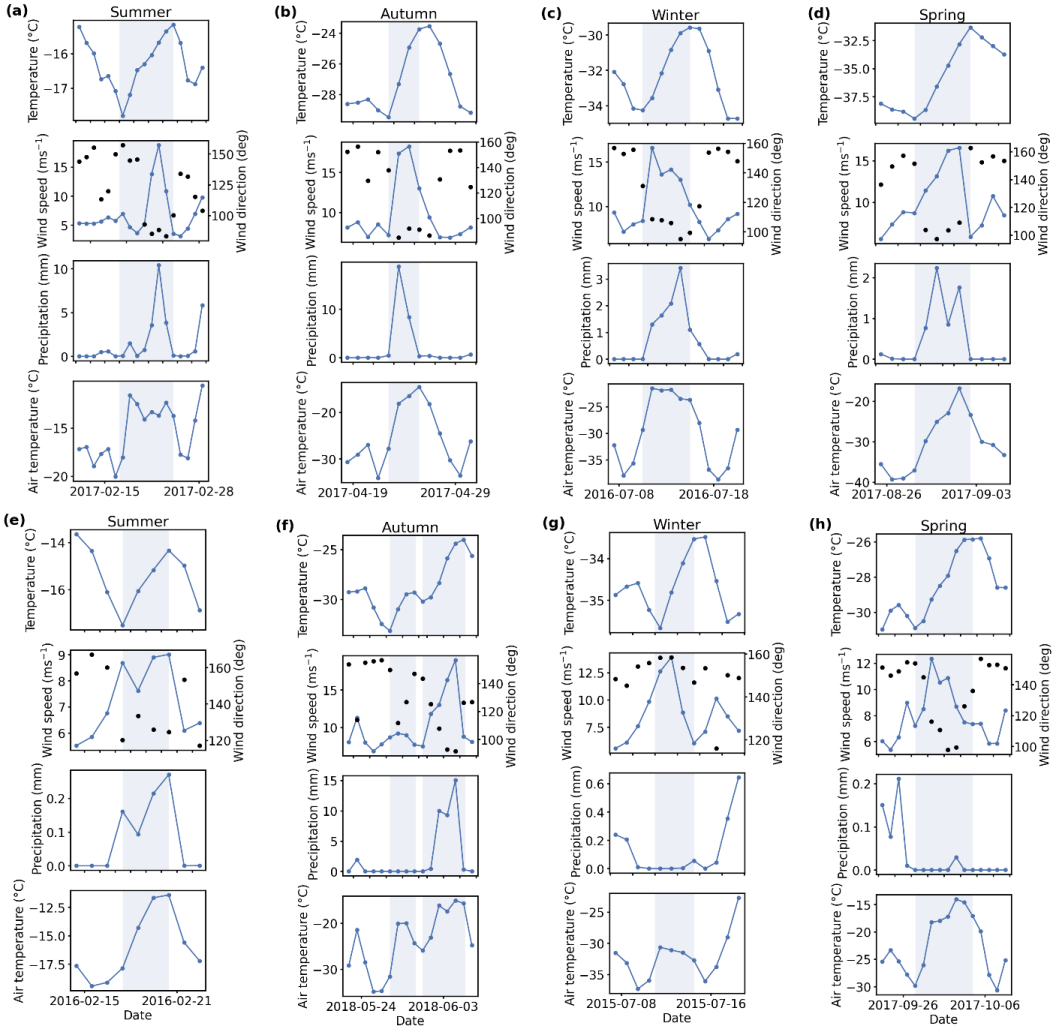

Figure 3: The time series of some ISSW events and their daily average meteorological conditions. The shaded region marks the beginning and end of each event. Onset is taken when the borehole temperature starts to increase and ends when the temperature stabilizes or decreases. In the order of panels, Surface temperature from the thermistor, wind speed and direction (as black dots), precipitation and 2m air temperature from ERA 5 for (a-d) Case 1 events for four seasons during 17-23 February 2017, 5-13 May 2018, 10-15 July 2016 and 28 August – 2 September 2017 (e-h) Case 2 events for four seasons during 17-20 February 2016, 27-30 May 2018 11-14 July 2015 and 27 September – 4 October 2017. A Case 1 event follows the event in autumn during 31 May-5 June 2018.

https://doi.org/10.5194/egusphere-2023-2515
Preprint. Discussion started: 15 December 2023

3.3 Ice sheet surface warming (ISSW) events

The daily averaged temperature at the borehole surface of location IND 33/B8 recorded during the period 2014–18 CE is presented in Fig. 4a. The dashed lines represent the ISSW events identified by criteria mentioned above. There were 71 significant warming events recorded for the period with a rise in temperature from 2 °C to 11 °C within 3 to 10 days of timespan. Yellow bar in Fig. 3b shows the number of events annually for the time period. It is evident that over this period, 2016 had the most number of warming events (18) followed by 2017 and 2018 (15 each). The year 2014 recorded the least number of events (8). Among these events throughout the entire study period from 2014 to 2018, the majority of events (49 ISSW events) were reported during spring (24) and winter (23), followed by autumn (14) and least during summer (8). January was the only month devoid of any ISSW events. Highest ISSW reported for the time period in thermistors was 11.7 °C and about 8 % of events were between 8 and 11.7 °C. The rest of the events (92 %) had warming below 8 °C. We examined the general meteorological conditions of the events. Out of 71 warming events, 60 were followed by snow precipitation, while the rest (11 events) were without any precipitation. Therefore, we assume the ISSW events with snow precipitation as Case 1 and ISSW events without snow precipitation as Case 2 to explain their respective features as follows:

Case 1: Figures 3 (a-d) show four case 1 events and their meteorological conditions. The events had high precipitation and surface wind speed (greater than average) with wind direction mostly easterlies. Here, the frequency increased from 10 (2015) to 16 (2016), but decreased to14 (2017) and 13 (2018) (Figure 4b). They occurred frequently during winter (21), spring (21), autumn (14) and summer (4) resulting in an average warming of ~4.6 °C in cDML ice sheets during 2014-18 with a maximum of 11 °C in October 2015.

Case 2: Figures 3 (e-g) give examples for four case 2 events that occurred during the period. Unlike the case 1 events, they had southeasterly winds without any precipitation. The event in Fig. 3f is later followed by a case 1 event featuring high easterly wind and precipitation. Here, the frequency was less with maximum number of events (4) in 2015 followed by 2018 (3), 2016 (2) and one each during 2014 and 2017 (Figure 4b). These events caused modest warming compared to Case 1, with maximum warming of 5 °C in October 2017. The frequency was maximum during summer and spring (4 each) followed by winter (2) and autumn (1).

https://doi.org/10.5194/egusphere-2023-2515
Preprint. Discussion started: 15 December 2023

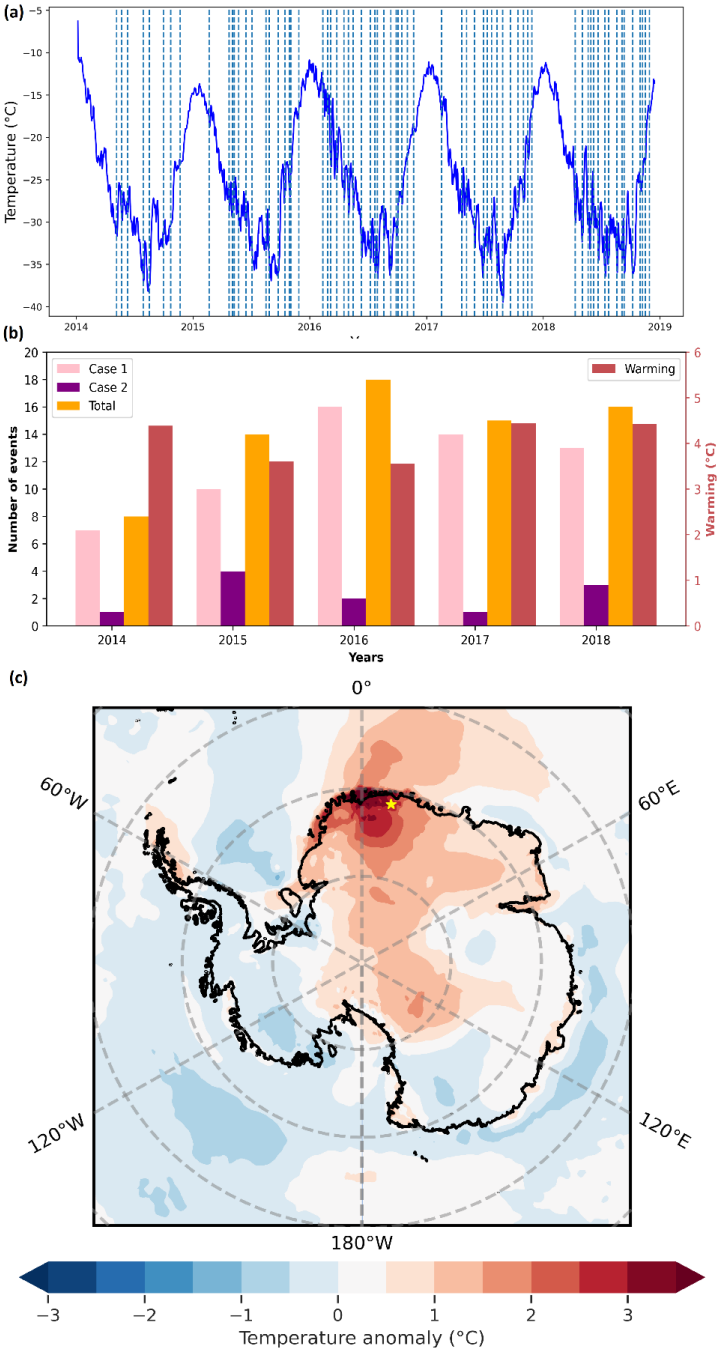

Figure 4: (a) Time series of daily average ice sheet surface temperature from borehole thermistors for the time period 2014-2018. Dashed lines represent the ISSW events. (b) The annual number of warming events and average ISSW caused by all the events during the study period. The color bars are; pink- case 1 events, violet – case 2 events and orange – the sum of

https://doi.org/10.5194/egusphere-2023-2515
Preprint. Discussion started: 15 December 2023

case 1 and case 2. (c) The composite of 2m air temperature anomaly for all the ISSW events from ERA5 dataset with respect to a 40 year climatology (1979-2019). The yellow star represents the borehole location.

Figure 4c gives the average of 2 m air temperature anomalies during the 71 ISSW events, with reference to a 40 year climatology (1979-2019). The spatial variation in average 2 m air temperature anomaly of all events generally showed higher temperature anomalies towards the coast, where the average warming was ~ 4 °C. This spatial variation suggests that regional-scale meteorological factors have greater control on the ISSW events.

3.4 Meteorological setting

As mentioned in Sect. 2.1, the surface winds over cDML were primarily katabatic (south-easterlies) with a mean wind speed of 8 ms^{-1} (Figure 1b & c). Due to their continental origin, they are colder and dryer. However, a fraction (~16 %) of wind blows from the east (Figure 1c) as well. The wind rose diagram for case 1 (Figure 5a) clearly indicates the dominant surface easterly winds (~ 32%) with the highest recorded wind speed of 25-30 ms^{-1}, suggesting that the case 1 events comprised the rare occasions of easterly wind events over the region. They had an average wind speed of 10 ms^{-1}, higher than the climatological mean wind speed (8 ms^{-1}). Since these winds are coming from the ocean, hence warmer and moist compared to the katabatic winds.

The wind rose diagram of case 2 (Figure 5d) has a different pattern from case 1 events. Southeasterly winds (katabatic) were present for 44 % of the time with maximum wind speed (>10 ms^{-1}) occurring at a frequency ~10 % higher than its climatological frequency (~1 %), suggesting the prevalence of strongest katabatic winds of the region. Hence, the general meteorological setting of the two cases were quite different due to the dominant easterly winds from the ocean for case 1 and strong SE winds (katabatic) for case 2. In the following sections, we look closely into the characteristics and mechanisms of ISSW episodes during the two events.

https://doi.org/10.5194/egusphere-2023-2515
Preprint. Discussion started: 15 December 2023

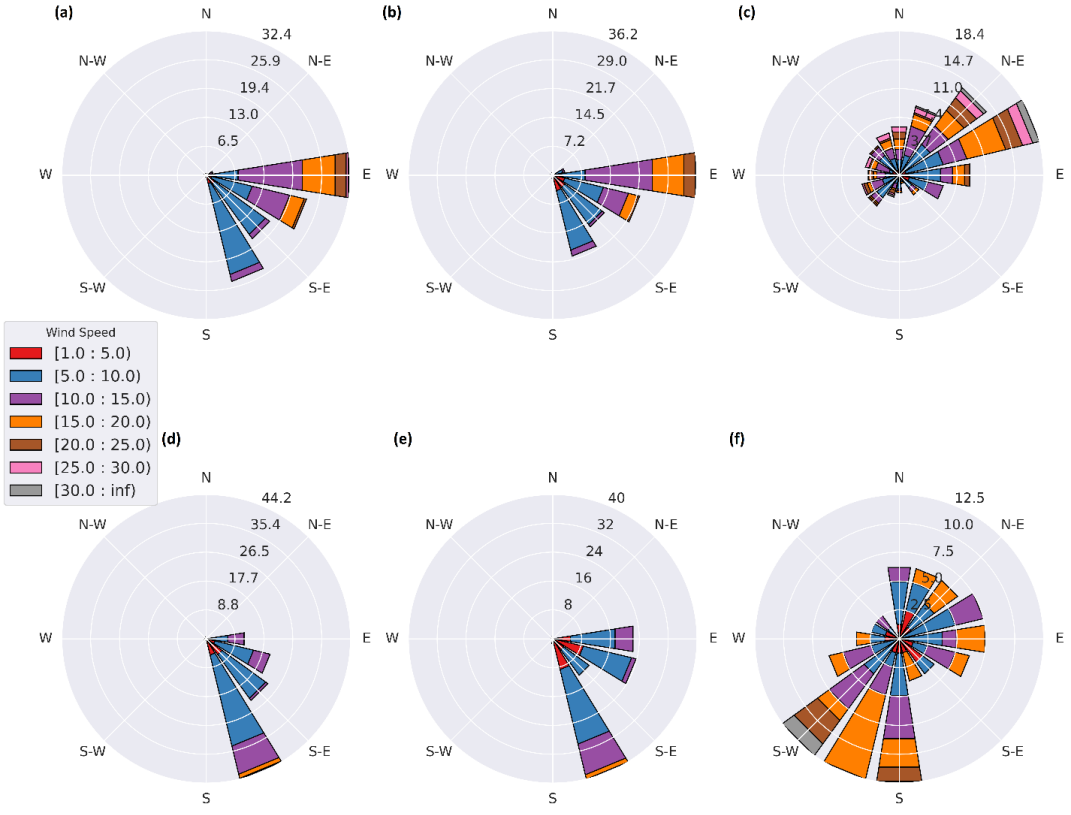

Figure 5: (a)-(c) Wind roses for case 1 at the surface, 850 hPa and 500 hPa, respectively, using ERA 5 data. (d)-(f) Wind roses for case 2 events at the surface, 850 hPa and 500 hPa, respectively, using ERA 5 data. Radial lines give the percentage of occurrence of wind in that particular direction. Color code represents wind speed with magnitude in the insect figure.

3.4.1 Mechanism for case 1 ISSW events

An examination of the surface energy balance for case 1 and 2 events will be useful to understand the mechanism of warming. The principle followed here is that the surface temperature increases coherently with increase in the net heat flux. Broadly, the net heat flux is affected by incoming and outgoing radiation and turbulent heat flux. To determine the major contributor to net heat flux in this case, we examined the correlations between daily net heat flux and its components during the case 1 events. The correlation between heat flux and net radiation was more significant (r = 0.54) than that between net flux and turbulent flux (r = 0.27), implying that the net radiation had more influence on net heat flux. The net radiation is the sum of net shortwave and longwave fluxes. The contribution of net shortwave radiation in net radiation for all the case 1 events (summer and winter combined) was very less (r = 0.37, $p<0.001$) compared to net longwave radiation (r = 0.67, $p<0.001$). Hence, a rise in net longwave radiation caused by high downward longwave radiation (LWD) could have increased the net heat flux. Thus, the surface warming of case 1 can be attributed to the high downward longwave radiation (LWD).

https://doi.org/10.5194/egusphere-2023-2515
Preprint. Discussion started: 15 December 2023

The LWD over a region depends on several factors such as the nature of cloud and air temperature (Sato and Simmonds, 2021). For most of the time, there were high cloud cover over the region during the events (Figure 6b). The wind at 850 hPa, and 500 hPa depict prominent easterly and north-easterly winds (Figure 5 b–c). Figure 6a represents the moisture flux during the events. There were significant northerly flow of moisture towards the region. The northerly winds carried warm, moist air from the surrounding ocean causing high cloud cover and LWD over the region. Warm air advection enhanced LWD by rising air temperature and cloud cover, resulting in surface warming. Studies have reported similar incidences of warming of air (Emanuelsson et al., 2018; Ghiz et al., 2021; Nicolas et al., 2017; Nicolas and Bromwich, 2011) and ice sheet surfaces (Sato and Simmonds, 2021) due to warm air advection from low latitudes.

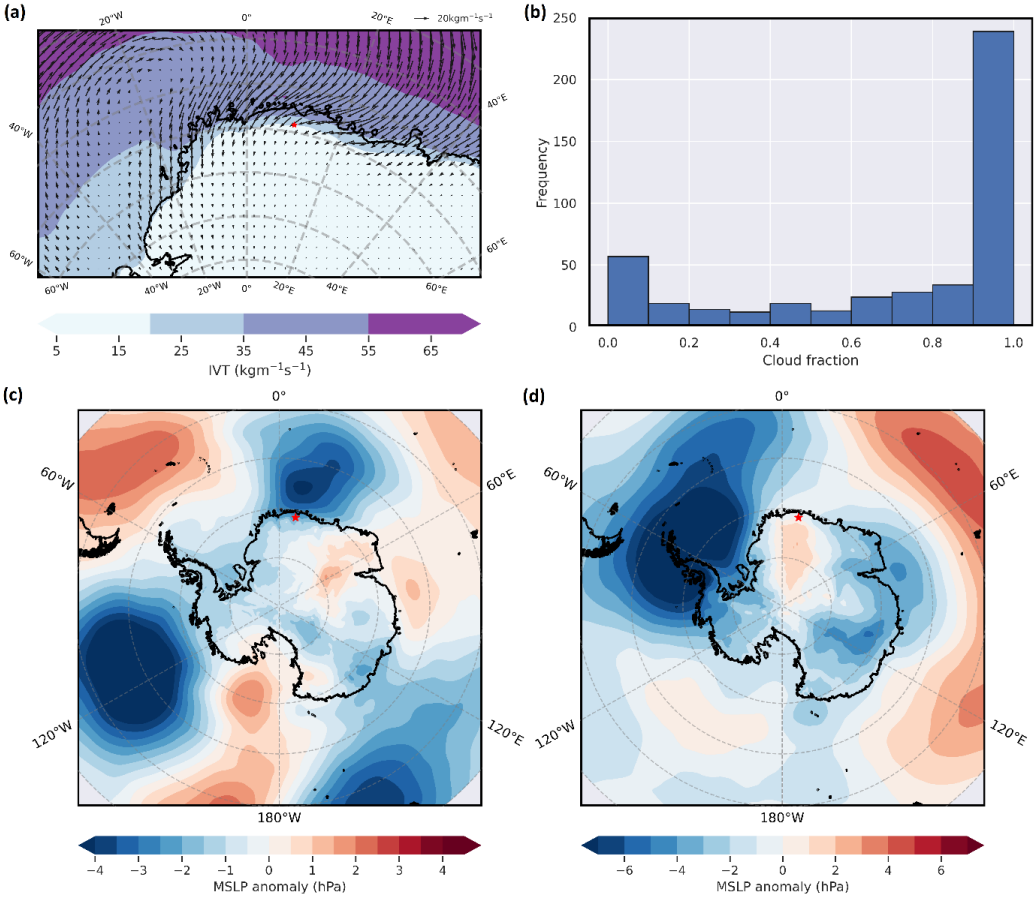

Figure 6: (a) Composite diagram of integrated moisture flux during case 1 events estimated from ERA 5. The arrow represents the direction and the color code gives the magnitude of moisture flux. Star shows the borehole location. (b) Histogram of cloud fraction during the case 1 events with the x-axis having cloud fraction and the y-axis having the frequency of occurrence of that particular cloud cover during case 1 events. Cloud fraction is obtained from ERA 5. (C)

https://doi.org/10.5194/egusphere-2023-2515
Preprint. Discussion started: 15 December 2023

Mean Sea Level Pressure anomaly for case 1 events, and (d) For case 2 events. Climatology is calculated for 1979-2018 from the ERA5 dataset.

In order to identify the causes of warm air advection, the composite of mean sea level pressure anomalies (MSLP) for case 1 is examined (Figure 6c). The synoptic arrangement over the continent resembled a wave number 3 pattern (3 lows and 3 highs). During the events, the region covering the location was inside a low-pressure system surrounded by high-pressure systems to the east and west. This particular synoptic condition favored the advection of warm, moist air to the region through the right side of the low-pressure area (Figure 6a).

3.4.2 Mechanism for case 2 ISSW events

For case 2, the intensity of warming was relatively less compared to case 1. On analyzing the energy balance in this case, we observed that net heat flux was greatly influenced by turbulent heat flux ($r = 0.37$, $p<0.001$) rather than net radiation ($r = 0.13$, $p = 0.01$), pointing out that turbulent flux has caused surface warming. Case 2 was influenced by the strong katabatic winds (Figure 5 d), where the upper-level winds were SE (850 hPa) and SW (500 hPa) respectively (Figure 5 (e-f)), suggesting that the winds were uniformly cold, still resulting in surface warming over the location. One plausible explanation could be the turbulence-induced disruption of thermal inversion by strong katabatic winds (Bromwich, 1989; Bromwich et al., 1993; Heinemann et al., 2019; King, 1998). During this process, warming is limited to a few heights above the surface, while the boundary layer is negatively buoyant (Bromwich, 1989). The MSLP anomaly for case 2 is different from the case 1, where there is a high pressure above the landmass flanked by low pressures on both sides (Figure 6d). This configuration of high and low pressure induces an anticyclonic circulation over the region, driving more southerly winds, further strengthening the katabatic winds and leading to surface warming.

4. Discussion

4.1 Insights in to the datasets used in the study: Advantages and limitations

The present work used ERA 5 reanalysis dataset to examine the surface and upper meteorological conditions over cDML. The availability, consistency and high spatial resolution makes ERA 5 an excellent choice for studying regions with limited data coverage like Antarctica. It is used in several studies to represent upper level meteorological conditions and accurately represent surface wind conditions (Tetzner et al., 2019). However, previous studies reported its biases in representing the near surface air temperature (Garza-Giron and Tulaczyk, 2023; Nielsen et al., 2023), while successfully representing general variability and trends (Zhu et al., 2021). We compared the daily mean 2m air temperature from a grid point near to borehole location with our borehole surface temperature and 2 m air temperature from a nearby station measurement (collected from Novolazarevskaya – Russia) for a year (Supplementary Figure 3s). From the figure it is evident that the profile of 2 m air temperature correlates well with borehole surface

https://doi.org/10.5194/egusphere-2023-2515
Preprint. Discussion started: 15 December 2023

temperature (r value = 0.851, $p < 0.001$) and with station 2 m temperature (r value = 0.932, $p < 0.001$). The station is situated coastal (~ 93 kms) and hence the temperature was warmer than borehole location.

Similar to other reanalysis datasets, previous studies reported bias in ERA 5 SEB fluxes over Antarctica due to limitations in the model physics (King et al., 2015). Silber et al (2019) observed biases in net SW and incoming LW fluxes by magnitudes ± 100 Wm^{-2} and ~50 Wm^{-2} respectively over West Antarctica in comparison with in situ measurements largely due to inaccurate representation of cloud phase in the model. To assess the accuracy of ERA 5 SEB fluxes over cDML near to our location, we compared it with monthly SEB fluxes from RACMO2.3p2. The monthly SEB fluxes of ERA 5 showed good correlation with monthly SEB fluxes from RACMO model near to borehole location (Supplementary Figure 4s). As mentioned before, the subsurface heat flux used in our study is derived from borehole thermistor measurements. It showed good agreement with RACMO model subsurface flux. Adding this derived subsurface flux to other SEB fluxes of ERA 5, the net heat flux is more accurate and correlates well with net heat flux of RACMO (Supplementary Figure 4s). Furthermore, we assessed daily SEB fluxes of ERA 5 using an AWS observation from to Larsen C Ice shelf in summer 2013 (Supplementary Figure 5s). Although the absolute values of ERA 5 deviated from observation, the overall pattern is mostly in agreement with in situ data. Ghiz et al (2021) observed qualitative consistency between in situ net energy flux and ERA5 over West Antarctica and therefore used ERA 5 SEB fluxes to assess the mechanism of melting events in their analysis. Since we limit ERA 5 temperature and SEB fluxes to a qualitative understanding of the events, we believe that the data represents the cases reasonably well for our study.

Accurate determination of ice sheet surface temperature is vital to understanding the impact of sudden atmospheric warming events on ice sheet surface energy balance, mass balance (through melting and sublimation) and subsurface temperature distribution. The temporal evolution of ISST is determined by the energy balance at the surface and near surface air temperature is only one contributor to it. Hence direct examination of ISST provides a better picture of the impact of these events on the Ice Sheet Surface rather than the 2 m air temperature measured by AWS. Compared with the skin temperature of ERA5, the borehole surface temperature had small amplitudes of day-to-day fluctuations, even though they followed a similar pattern as that of 2 m air temperature (Supplementary Figure 3s). This dampening of temperature fluctuations over the Ice Sheet surface compared to near surface air is obvious and borehole thermistors provided a more realistic behavior of the Ice sheet surface. In addition, the yearly mean values during 2015 were -24.43 °C and -25.15 °C for borehole and ERA5 surface temperatures respectively, indicating cold bias in ERA 5 skin temperature.

Satellite derived land surface temperature is an excellent tool for studying ISST due to its large spatial coverage, however, it is limited to clear sky conditions over Antarctica. We observe from our study that borehole thermistor measurements can be used to conduct a year-round study of ISST and accurately derive ground heat flux. They can also serve as a ground truth for satellite observations.

4.2 Ice sheet surface warming and linkage to Atmospheric circulation in cDML

The spatial and temporal changes in the ice sheet surface temperature are interlinked to several divers in the atmosphere such as clouds and winds. The regional changes are modified in a complex way by the strength and path

https://doi.org/10.5194/egusphere-2023-2515
Preprint. Discussion started: 15 December 2023

of individual storm tracks around the cDML region, which has a greater role in the ice sheet surface warming and accumulation. Two factors have been identified as drivers of ISSW events over cDML region for the period 2014-18. The major factor is the strong easterly winds favoring high snow accumulation (case 1, 60 events). This is driven by advection of warm, moist air from the ocean. The southern ocean is a region of high storm activity at all times of year (Hoskins and Hodges, 2005) that witnessed increased cyclone events due to global warming (Reboita et al., 2015). The increased cyclones in the southern hemisphere, irrespective of the season, could also influence the ISSW events over the cDML region.

Case 1 has shown warming for a few days in the range of 2 – 11 °C with an average warming of ~4.6 °C due to high LWD. The events were episodic with high interannual and intra-seasonal variability. The frequency has increased from 8 to 16 events per year after 2015, with maximum during 2016 (16) followed by 2017 (14) and 2018 (13). It can also be seen that even within a year, the frequency was more during winter and spring compared to summer. The influence of LWD on ice sheet warming depends on the cloud optical thickness, liquid water path (LWP) and cloud phase (Wille et al., 2019; Bennartz et al., 2013; Nicolas et al., 2017). Changes in any of these parameters can alter the LWD and thereby the extent of warming. Kittel et al (2022) projected extensive melting of Antarctic ice shelves by increased liquid water in clouds via radiation perturbations. Therefore major uncertainty in surface warming is related to the increase of low-level liquid clouds which would emit more LWD leading to surface warming (Bennartz et al., 2013; Hofer et al., 2019; Gorodetskaya et al., 2015).

Case 2 (11 events) was associated with katabatic winds (SE) with no precipitation, causing a relatively modest warming in the range of 2-5 °C over the region (average warming of ~3.62 °C). During the events, the usual winds were strengthened by a peculiar synoptic configuration of high pressure over the location and low pressure to both sides, causing very strong katabatic winds (>10 ms^{-1}), which resulted in a cold, dry air blowing from the continent to the coast. The strong katabatic winds eventually intensified turbulent flux to warm the ice surface adiabatically (Bromwich, 1989). The warming due to katabatic wind is dependent on the wind speed (Vihma et al., 2011); hence any changes in wind speed can affect the warming (Nylen et al., 2004; Speirs et al., 2010; Vihma et al., 2011). Warming and exposure of low albedo ice layers due to persistent katabatic wind scouring have led to surface melting over a cDML ice shelf (Lenaerts et al., 2017). It is also established that katabatic winds, in association with synoptic systems and topographic channeling, often lead to warming of the Antarctic glaciers (Bromwich et al., 1993; Heinemann et al., 2019). The katabatic winds is an important climatological signal (mean warm anomaly > 5 K for > 120 days) during winter in the Byrd Glacier and the Nimrod Glacier (Heinemann et al., 2019). These winds might expose blue ice and firn of less surface albedo, and enhance melt over the cDML region as well. Such episodic interactions of synoptic systems with the persistent katabatic winds might create additional pressures at the ice sheet surface such as wind scouring, sublimation and surface melting.

4.3 Warming of ice sheet surface and linkages to precipitation

https://doi.org/10.5194/egusphere-2023-2515
Preprint. Discussion started: 15 December 2023

The case 1 warming events have witnessed high snow accumulation in the region caused by cyclonic disturbances. 35 out of the total 60 events in case 1 experienced extreme precipitation (EPEs), where the daily precipitation was greater than the 90th percentile of the study period (2014-18). The average frequency was 7 events per year, in agreement with Schlosser et al. (2010) observing an average frequency of 8 events per year in western DML during 2001-06. The moisture transport efficiency of cyclones is dependent on the genesis latitude and speed of their poleward propagation (Sinclair and Dacre, 2019). Low latitude origin and high propagation velocity of cyclones can transport more moisture towards Antarctica. Several studies have emphasized the role of atmospheric rivers - narrow bands of moist air from low latitudes – in bringing extreme precipitation to the Polar region and causing surface melt by enhancing longwave radiation associated with its optically thick clouds (Gorodetskaya et al., 2014; Wille et al., 2019). Therefore, the high snow precipitation during case 1 could have resulted from an intense long-range meridional moisture transport from low latitudes and the surrounding ocean. Hence it is likely that changes in the source (latitude), frequency, intensity and transport efficiency of cyclones directly affect the precipitation regime over cDML and indirectly affect ISSW by its cloud cover. A future perspective of this study will be examining and quantifying their role in ISSW events.

4.4 Implications of ISSW events in cDML

The extent of warming due to katabatic winds are modest in the region compared to case 1 events, though very strong katabatic winds can create additional effects on the ice sheet by drifting and sublimating the accumulated snow and exposing low albedo ice (Van Den Broeke, 1997; Ligtenberg et al., 2014; Lenaerts et al., 2017). Our estimated average sublimation rate of cDML for the five years is 0.17 mm per day, which is comparable to the rates estimated using AWS in eastern Dronning Maud Land (Van Den Broeke et al., 2004, 2009). During the case 2 events, however, it increased to a mean of 0.27 mm per day, signifying the role of dry katabatic winds on sublimation. Surface sublimation affects the mass balance of ice sheets by removing the precipitation (Barral et al., 2014; Grazioli et al., 2017) and altering the composition of ice cores (Masson-Delmotte et al., 2008). Additionally, such events might impact the southern ocean by drifting the sea ice (Farooq et al., 2023; Aulicino et al., 2019) and creating coastal polynyas (Bromwich et al., 1993; Ebner et al., 2014). This has a consequence on the biological productivity of the Southern ocean (Montes-Hugo et al., 2009) and CO_2 uptake. In summer, such regional surface warming events might raise the ISST to melt threshold (0 °C) and lead to surface melting. Additionally, strong winds associated with them can potentially erode the snow and increase surface melt. This could result in the supraglacial and englacial storage of meltwater at the ice-sheet grounding zone of East Antarctica, which could affect the hydrodynamics of ice sheet in the future.

The present study did not observe any melting near the borehole location as the temperatures were subzero even in summer. However, considering the spatial extent of these warming episodes (Figure 2c), surface melting could be observed over the ice shelves towards the coast during summer. There are studies on the melt layers captured in ice cores retrieved from coastal regions of Antarctica, including DML (Dey et al., 2022; Kaczmarska et al., 2006). Such melt layers cause changes in the physical and chemical properties of ice and affect their interpretation with past

https://doi.org/10.5194/egusphere-2023-2515
Preprint. Discussion started: 15 December 2023

climate (Pohjola et al., 2002). Moreover, frequent surface melting create melt ponds (Luckman et al., 2014; Scambos et al., 2000) and subsequent depletion of firn air can lead to hydrofracture of ice shelves (Banwell et al., 2013; Scambos et al., 2000). Similar scenarios were previously observed over the Antarctic Peninsula (Banwell et al., 2013; Scambos et al., 2000). The extent of firn air depletion can be buffered by accumulation that replenishes free pore space required to hold meltwater (Ligtenberg et al., 2011). All the major warming events observed in the present study were associated with snow accumulation, reducing the risk of any firn air depletion. However, the snow accumulation estimated from an ice core drilled in the exact location (Ejaz et al., 2021) revealed a decreasing trend in accumulation over the last century (53 % during 1906-2013 CE) dropping to 20 % since 2000 CE (Supplementary Figure 6s). Further, a sharp decrease of snow accumulation along with high melt events would result in firn air depletion over cDML, which may cause a major hydro-facture of the ice shelves in the cDML region in the future. Hence, a continuation of this study over a long term will help to identify the impact of frequency and duration of such warming events and accumulation patterns to predict the stability of ice shelves in a better way.

5. Conclusion

Using thermistors deployed in an ice core borehole, we examined the warming events of coastal Dronning Maud land region during 2014-2018. Local changes in surface energy balance and large-scale atmospheric circulation were found to warm the surface continuously for several degrees for some days in cDML. There were 71 ISSW events following the selection criteria in the study period, occurring in all seasons in the order spring>winter >autumn>summer with an the mean amplitude of spontaneous warming events that continue for a few days by about 4.1 °C during 2014-2018 CE. The study identified two major drivers of warming over the region. The majority of the ISSW events (84 %) were associated with warm air advection and enhanced cloud-induced downward longwave radiation along with snow precipitation during high easterlies (case 1 events) and the rest with southeasterly winds devoid of any precipitation (case 2 events). Strong surface easterly winds and precipitation accompanied Case 1 events, whereas case 2 events were associated with turbulence caused by strong katabatic winds at the surface. Our study suggests that short-term surface warming events of cDML are driven by local changes in surface energy balance favored by large-scale atmospheric circulations. The frequency and duration of such events are important for the stability and mass balance of coastal Antarctic ice shelves.

Data availability

The data used in this work is available at http://ramadda.npdc.ncpor.res.in/repository/entry/show?entryid=a9bcd8a3-7417-4bad-bd1e-44ecf1b8ad69. It include the six hourly dataset of borehole thermistor measurements from cDML for 2014-2018 from a height of 1.2m to a depth of 30m. ERA5 data can be downloaded from Copernicus Climate Data store provided by ECMWF (https://doi.org/10.24381/cds.f17050d7, Hersbach et al., 2020). RACMO.3p2 model output is obtained from Zenodo data repository in monthly scale with a spatial resolution of 27 km (DOI 10.5281/zenodo.7760490, van Wessem et al., 2023). The daily SEB fluxes from an AWS in Larsen C ice shelf is available on PANGEA database (https://doi.org/10.1594/PANGAEA.910471, Jakobs et al., 2020). Novolazarskaya

https://doi.org/10.5194/egusphere-2023-2515
Preprint. Discussion started: 15 December 2023

station observation is collected as part of READER project and is available on ftp://ftp.bas.ac.uk/src/ANTARCTIC_METEOROLOGICAL_DATA/GTS_DATA/SURFACE/ (Turner et al., 2004).

Author contribution

Gayathri E M: Sampling, Methodology, Data Curation, Formal analysis, Writing - Original Draft. **Laluraj C M:** Conceptualization, Methodology, Writing - Review & Editing, **Satheesan k:** Validation, Writing – Review & Editing. **Kenichi Matsuoka:** Supervision, Conceptualization, Review & Editing. **Thamban Meloth:** Project administration.

Competing interests

The authors do not have any competing interests.

Acknowledgements

We thank the Ministry of Earth Sciences for financial support through the project 'PACER - Cryosphere and Climate'. We express our gratitude to Mr. Bhikaji L Redkar and Dr Mahalinganathan K for deploying the instrument in the field. This is NCPOR contribution No. xxx.

References

Altnau, S., Schlosser, E., Isaksson, E., and Divine, D.: Climatic signals from 76 shallow firn cores in Dronning Maud Land, East Antarctica, Cryosphere, 9, 925–944, https://doi.org/10.5194/tc-9-925-2015, 2015.

Aulicino, G., Wadhams, P., and Parmiggiani, F.: SAR Pancake Ice thickness retrieval in the Terra Nova Bay (Antarctica) during the PIPERS expedition in Winter 2017, Remote Sens., 11, https://doi.org/10.3390/rs11212510, 2019.

Banwell, A. F., MacAyeal, D. R., and Sergienko, O. V.: Breakup of the Larsen B Ice Shelf triggered by chain reaction drainage of supraglacial lakes, Geophys. Res. Lett., 40, 5872–5876, https://doi.org/10.1002/2013GL057694, 2013.

Barral, H., Genthon, C., Trouvilliez, A., Brun, C., and Amory, C.: Blowing snow in coastal Adélie Land, Antarctica: three atmospheric-moisture issues, Cryosph., 8, 1905–1919, 2014.

Bennartz, R., Shupe, M. D., Turner, D. D., Walden, V. P., Steffen, K., Cox, C. J., Kulie, M. S., Miller, N. B., and Pettersen, C.: July 2012 Greenland melt extent enhanced by low-level liquid clouds, Nature, 496, 83–86, 2013.

Bozkurt, D., Rondanelli, R., Marín, J. C., and Garreaud, R.: Foehn Event Triggered by an Atmospheric River Underlies Record-Setting Temperature Along Continental Antarctica, J. Geophys. Res. Atmos., 123, 3871–3892, https://doi.org/10.1002/2017JD027796, 2018.

https://doi.org/10.5194/egusphere-2023-2515
Preprint. Discussion started: 15 December 2023

Brandt, R. E. and Warren, S. G.: Solar-heating rates and temperature profiles in Antarctic snow and ice, J. Glaciol., 39, 99–110, https://doi.org/10.3189/S0022143000015756, 1993.

Van Den Broeke, M. R.: Spatial and temporal variation of sublimation on Antarctica: Results of a high-resolution general circulation model, J. Geophys. Res. Atmos., 102, 29765–29777, https://doi.org/10.1029/97JD01862, 1997.

Van Den Broeke, M. R., Reijmer, C. H., and Van De Wal, R. S. W.: A study of the surface mass balance in Dronning Maud Land, Antarctica, using automatic weather stationS, 2004.

van den Broeke, M.: Strong surface melting preceded collapse of Antarctic Peninsula ice shelf, Geophys. Res. Lett., 32, 1–4, https://doi.org/10.1029/2005GL023247, 2005.

Van Den Broeke, M., König-Langlo, G., Picard, G., Kuipers Munneke, P., and Lenaerts, J.: Surface energy balance, melt and sublimation at Neumayer Station, East Antarctica, Antarct. Sci., 22, 87–96, https://doi.org/10.1017/S0954102009990538, 2009.

Bromwich, D. H.: Satellite Analyses of Antarctic Katabatic Wind Behavior, Bull. Am. Meteorol. Soc., 70, 738–749, https://doi.org/10.1175/1520-0477(1989)070<0738:SAOAKW>2.0.CO;2, 1989.

Bromwich, D. H., Carrasco, J. F., Zhong Liu, and Ren-Yow Tzeng: Hemispheric atmospheric variations and oceanographic impacts associated with katabatic surges across the Ross ice shelf, Antarctica, J. Geophys. Res. Atmos., 98, 13045–13062, https://doi.org/10.1029/93JD00562, 1993.

Cape, M. R., Vernet, M., Skvarca, P., Marinsek, S., Scambos, T., and Domack, E.: Foehn winds link climate-driven warming to ice shelf evolution in Antarctica, J. Geophys. Res. Atmos., 120, 11,037-11,057, https://doi.org/10.1002/2015JD023465, 2015.

Dey, R., Thamban, M., Laluraj, C. M., Mahalinganathan, K., Redkar, B. L., Kumar, S., and Matsuoka, K.: Application of visual stratigraphy from line-scan images to constrain chronology and melt features of a firn core from coastal Antarctica, J. Glaciol., 1–12, https://doi.org/10.1017/JOG.2022.59, 2022.

Ebner, L., Heinemann, G., Haid, V., and Timmermann, R.: Katabatic winds and polynya dynamics at Coats Land, Antarctica, Antarct. Sci., 26, 309–326, https://doi.org/10.1017/S0954102013000679, 2014.

Ejaz, T., Rahaman, W., Laluraj, C. M., Mahalinganathan, K., and Thamban, M.: Sea Ice Variability and Trends in the Western Indian Ocean Sector of Antarctica During the Past Two Centuries and Its Response to Climatic Modes, J. Geophys. Res. Atmos., 126, 1–23, https://doi.org/10.1029/2020JD033943, 2021.

Emanuelsson, B. D., Bertler, N. A. N., Neff, P. D., Renwick, J. A., Markle, B. R., Baisden, W. T., and Keller, E. D.: The role of Amundsen–Bellingshausen Sea anticyclonic circulation in forcing marine air intrusions into West Antarctica, Clim. Dyn., 51, 3579–3596, https://doi.org/10.1007/S00382-018-4097-3/FIGURES/10, 2018.

https://doi.org/10.5194/egusphere-2023-2515
Preprint. Discussion started: 15 December 2023

Farooq, U., Rack, W., McDonald, A., and Howell, S.: Representation of sea ice regimes in the Western Ross Sea, Antarctica, based on satellite imagery and AMPS wind data, Clim. Dyn., 60, 227–238, https://doi.org/10.1007/s00382-022-06319-9, 2023.

Garza-Giron, R. and Tulaczyk, S. M.: Brief communication: Significant cold bias in ERA5 output for McMurdo region, Antarctica, Cryosph. Discuss., 2023, 1–10, https://doi.org/10.5194/tc-2023-44, 2023.

Ghiz, M. L., Scott, R. C., Vogelmann, A. M., Lenaerts, J. T. M., Lazzara, M., and Lubin, D.: Energetics of surface melt in West Antarctica, Cryosphere, 15, 3459–3494, https://doi.org/10.5194/TC-15-3459-2021, 2021.

Goel, V., Matsuoka, K., Berger, C. D., Lee, I., Dall, J., and Forsberg, R.: Characteristics of ice rises and ice rumples in Dronning Maud Land and Enderby Land, Antarctica, J. Glaciol., 66, 1064–1078, https://doi.org/DOI: 10.1017/jog.2020.77, 2020.

Gorodetskaya, I. V., Tsukernik, M., Claes, K., Ralph, M. F., Neff, W. D., and Van Lipzig, N. P. M.: The role of atmospheric rivers in anomalous snow accumulation in East Antarctica, Geophys. Res. Lett., 41, 6199–6206, https://doi.org/10.1002/2014GL060881, 2014.

Gorodetskaya, I. V, Kneifel, S., Maahn, M., Van Tricht, K., Thiery, W., Schween, J. H., Mangold, A., Crewell, S., and Van Lipzig, N. P. M.: Cloud and precipitation properties from ground-based remote-sensing instruments in East Antarctica, Cryosph., 9, 285–304, 2015.

Grazioli, J., Madeleine, J. B., Gallée, H., Forbes, R. M., Genthon, C., Krinner, G., and Berne, A.: Katabatic winds diminish precipitation contribution to the Antarctic ice mass balance, Proc. Natl. Acad. Sci. U. S. A., 114, 10858–10863, https://doi.org/10.1073/PNAS.1707633114/SUPPL_FILE/PNAS.201707633SI.PDF, 2017.

Heinemann, G.: On the streakiness of katabatic wind signatures on high-resolution AVHRR satellite images: Results from the aircraft-based experiment KABEG, Polarforschung, 66, 19–30, 2000.

Heinemann, G., Glaw, L., and Willmes, S.: A Satellite-Based Climatology of Wind-Induced Surface Temperature Anomalies for the Antarctic, Remote Sens., 11, 1539, https://doi.org/10.3390/RS11131539, 2019.

Hersbach, H., Bell, B., Berrisford, P., Hirahara, S., Horányi, A., Muñoz-Sabater, J., Nicolas, J., Peubey, C., Radu, R., Schepers, D., Simmons, A., Soci, C., Abdalla, S., Abellan, X., Balsamo, G., Bechtold, P., Biavati, G., Bidlot, J., Bonavita, M., De Chiara, G., Dahlgren, P., Dee, D., Diamantakis, M., Dragani, R., Flemming, J., Forbes, R., Fuentes, M., Geer, A., Haimberger, L., Healy, S., Hogan, R. J., Hólm, E., Janisková, M., Keeley, S., Laloyaux, P., Lopez, P., Lupu, C., Radnoti, G., de Rosnay, P., Rozum, I., Vamborg, F., Villaume, S., and Thépaut, J. N.: The ERA5 global reanalysis, Q. J. R. Meteorol. Soc., 146, 1999–2049, https://doi.org/10.1002/qj.3803, 2020.

Hirasawa, N., Nakamura, H., and Yamanouchi, T.: Abrupt changes in meteorological conditions observed at an

https://doi.org/10.5194/egusphere-2023-2515
Preprint. Discussion started: 15 December 2023

inland Antarctic Station in association with wintertime blocking, Geophys. Res. Lett., 27, 1911–1914, https://doi.org/10.1029/1999GL011039, 2000.

Hofer, S., Tedstone, A. J., Fettweis, X., and Bamber, J. L.: Cloud microphysics and circulation anomalies control differences in future Greenland melt, Nat. Clim. Chang., 9, 523–528, 2019.

Hoskins, B. J. and Hodges, K. I.: A new perspective on Southern Hemisphere storm tracks, J. Clim., 18, 4108–4129, 2005.

Hui, F., Ci, T., Cheng, X., Scambo, T. A., Liu, Y., Zhang, Y., Chi, Z., Huang, H., Wang, X., and Wang, F.: Mapping blue-ice areas in Antarctica using ETM+ and MODIS data, Ann. Glaciol., 55, 129–137, 2014.

Jakobs, C. L., Reijmer, C. H., van den Broeke, M. R., Smeets, P., and König-Langlo, G.: High-resolution meteorological observations, Surface Energy Balance components and miscellaneous data from AWS IMAU_aws15, https://doi.org/10.1594/PANGAEA.910471, 8 January 2020.

Kaczmarska, M., Isaksson, E., Karlöf, L., Brandt, O., Winther, J. G., Van De Wal, R. S. W., Van Den Broeke, M., and Johnsen, S. J.: Ice core melt features in relation to Antarctic coastal climate, Antarct. Sci., 18, 271–278, https://doi.org/10.1017/S0954102006000319, 2006.

KIKUCHI, T., SATOW, K., OH ATA, T., YAMANOUCHI, T., and NISHIO, F.: Wind and temperature regime in Mizuho Plateau, East Antarctica, Int. J. Remote Sens., 13, 67–79, https://doi.org/10.1080/01431169208904026, 1992.

King, J. C., Gadian, A., Kirchgaessner, A., Kuipers Munneke, P., Lachlan-Cope, T. A., Orr, A., Reijmer, C., Van Den Broeke, M. R., Van Wessem, J. M., and Weeks, M.: Validation of the summertime surface energy budget of Larsen C Ice Shelf (Antarctica) as represented in three high-resolution atmospheric models, J. Geophys. Res. Atmos., 120, 1335–1347, 2015.

King, J. C., Kirchgaessner, A., Bevan, S., Elvidge, A. D., Kuipers Munneke, P., Luckman, A., Orr, A., Renfrew, I. A., and van den Broeke, M. R.: The Impact of Föhn Winds on Surface Energy Balance During the 2010–2011 Melt Season Over Larsen C Ice Shelf, Antarctica, J. Geophys. Res. Atmos., 122, 12,062-12,076, https://doi.org/10.1002/2017JD026809, 2017.

KING, J. C.: Using satellite thermal infrared imagery to study boundary layer structure in an Antarctic katabatic wind region, Int. J. Remote Sens., 19, 3335–3348, https://doi.org/10.1080/014311698214028, 1998.

Kittel, C., Amory, C., Hofer, S., Agosta, C., Jourdain, N. C., Gilbert, E., Le Toumelin, L., Vignon, É., Gallée, H., and Fettweis, X.: Clouds drive differences in future surface melt over the Antarctic ice shelves, Cryosph., 16, 2655–2669, https://doi.org/10.5194/tc-16-2655-2022, 2022.

https://doi.org/10.5194/egusphere-2023-2515
Preprint. Discussion started: 15 December 2023

Kreutz, K. J., Mayewski, P. A., Pittalwala, I. I., Meeker, L. D., Twickler, M. S., and Whitlow, S. I.: Sea level pressure variability in the Amundsen Sea region inferred from a West Antarctic glaciochemical record, J. Geophys. Res. Atmos., 105, 4047–4059, 2000.

Lenaerts, J. T. M., van Meijgaard, E., van den Broeke, M. R., Ligtenberg, S. R. M., Horwath, M., and Isaksson, E.: Recent snowfall anomalies in Dronning Maud Land, East Antarctica, in a historical and future climate perspective, Geophys. Res. Lett., 40, 2684–2688, 2013.

Lenaerts, J. T. M., Brown, J., Van Den Broeke, M. R., Matsuoka, K., Drews, R., Callens, D., Philippe, M., Gorodetskaya, I. V, Van Meijgaard, E., and Reijmer, C. H.: High variability of climate and surface mass balance induced by Antarctic ice rises, J. Glaciol., 60, 1101–1110, 2014.

Lenaerts, J. T. M., Lhermitte, S., Drews, R., Ligtenberg, S. R. M., Berger, S., Helm, V., Smeets, C. J. P. P., Broeke, M. R. V. Den, Van De Berg, W. J., Van Meijgaard, E., Eijkelboom, M., Eisen, O., and Pattyn, F.: Meltwater produced by wind–albedo interaction stored in an East Antarctic ice shelf, Nat. Clim. Chang., 7, 58–62, https://doi.org/10.1038/nclimate3180, 2017.

Ligtenberg, S. R. M., Helsen, M. M., and Van den Broeke, M. R.: An improved semi-empirical model for the densification of Antarctic firn, Cryosph., 5, 809–819, 2011.

Ligtenberg, S. R. M., Lenaerts, J. T. M., Van Den Broeke, M. R., and Scambos, T. A.: On the formation of blue ice on Byrd Glacier, Antarctica, J. Glaciol., 60, 41–50, https://doi.org/10.3189/2014JOG13J116, 2014.

Lindbäck, K., Moholdt, G., Nicholls, K. W., Hattermann, T., Pratap, B., Thamban, M., and Matsuoka, K.: Spatial and temporal variations in basal melting at Nivlisen ice shelf, East Antarctica, derived from phase-sensitive radars, Cryosph., 13, 2579–2595, 2019.

Lowther, A., von Quillfeldt, C., Assmy, P., De Steur, L., Descamps, S., Divine, D., Elvevold, S., Forwick, M., Fransson, A., Fraser, A., Gerland, S., Granskog, M., Hallanger, I., Hattermann, T., Itkin, M., Hop, H., Husum, K., Kovacs, K., Lydersen, C., Matsuoka, K., Miettinen, A., Moholdt, G., Moreau, S., Myhre, P. I., Orme, L., Pavlova, O., and Tandberg, A. H.: A review of the scientific knowledge of the seascape off Dronning Maud Land, Antarctica, https://doi.org/10.1007/s00300-022-03059-8, 1 August 2022.

Luckman, A., Elvidge, A., Jansen, D., Kulessa, B., Kuipers Munneke, P., King, J., and Barrand, N. E.: Surface melt and ponding on Larsen C Ice Shelf and the impact of föhn winds, Antarct. Sci., 26, 625–635, https://doi.org/10.1017/S0954102014000339, 2014.

Massom, R. A., Pook, M. J., Comiso, J. C., Adams, N., Turner, J., Lachlan-Cope, T., and Gibson, T. T.: Precipitation over the interior East Antarctic ice sheet related to midlatitude blocking-high activity, J. Clim., 17, 1914–1928, 2004.

https://doi.org/10.5194/egusphere-2023-2515
Preprint. Discussion started: 15 December 2023

Masson-Delmotte, V., Hou, S., Ekaykin, A., Jouzel, J., Aristarain, A., Bernardo, R. T., Bromwich, D., Cattani, O., Delmotte, M. M., Falourd, S., Frezzotti, M., Gallée, H., Genoni, L., Isaksson, E., Landais, A., Helsen, M. M., Hoffmann, G., Lopez, J., Morgan, V., Motoyama, H., Noone, D., Oerter, H., Petit, J. R., Royer, A., Uemura, R., Schmidt, G. A., Schlosser, E., Simões, J. C., Steig, E. J., Stenni, B., Stievenard, M., Van Den Broeke, M. R., Van De Wal, R. S. W., Van De Berg, W. J., Vimeux, F., and White, J. W. C.: A Review of Antarctic Surface Snow Isotopic Composition: Observations, Atmospheric Circulation, and Isotopic Modeling, J. Clim., 21, 3359–3387, https://doi.org/10.1175/2007JCLI2139.1, 2008.

Matsuoka, K., Hindmarsh, R. C. A., Moholdt, G., Bentley, M. J., Pritchard, H. D., Brown, J., Conway, H., Drews, R., Durand, G., Goldberg, D., Hattermann, T., Kingslake, J., Lenaerts, J. T. M., Martín, C., Mulvaney, R., Nicholls, K. W., Pattyn, F., Ross, N., Scambos, T., and Whitehouse, P. L.: Antarctic ice rises and rumples: Their properties and significance for ice-sheet dynamics and evolution, Earth-Science Rev., 150, 724–745, https://doi.org/https://doi.org/10.1016/j.earscirev.2015.09.004, 2015.

Matsuoka, K., Skoglund, A., Roth, G., de Pomereu, J., Griffiths, H., Headland, R., Herried, B., Katsumata, K., Le Brocq, A., and Licht, K.: Quantarctica, an integrated mapping environment for Antarctica, the Southern Ocean, and sub-Antarctic islands, Environ. Model. Softw., 140, 105015, 2021.

Montes-Hugo, M., Doney, S. C., Ducklow, H. W., Fraser, W., Martinson, D., Stammerjohn, S. E., and Schofield, O.: Recent changes in phytoplankton communities associated with rapid regional climate change along the western Antarctic Peninsula, Science (80-.)., 323, 1470–1473, https://doi.org/10.1126/science.1164533, 2009.

Nicolas, J. P. and Bromwich, D. H.: Climate of West Antarctica and Influence of Marine Air Intrusions, J. Clim., 24, 49–67, https://doi.org/10.1175/2010JCLI3522.1, 2011.

Nicolas, J. P., Vogelmann, A. M., Scott, R. C., Wilson, A. B., Cadeddu, M. P., Bromwich, D. H., Verlinde, J., Lubin, D., Russell, L. M., Jenkinson, C., Powers, H. H., Ryczek, M., Stone, G., and Wille, J. D.: January 2016 extensive summer melt in West Antarctica favoured by strong El Niño, Nat. Commun., 8, 1–10, https://doi.org/10.1038/ncomms15799, 2017.

Nielsen, E. B., Katurji, M., Zawar-Reza, P., and Meyer, H.: Antarctic daily mesoscale air temperature dataset derived from MODIS land and ice surface temperature, Sci. Data, 10, 833, https://doi.org/10.1038/s41597-023-02720-z, 2023.

Noone, D., Turner, J., and Mulvaney, R.: Atmospheric signals and characteristics of accumulation in Dronning Maud Land, Antarctica, J. Geophys. Res. Atmos., 104, 19191–19211, 1999.

Nylen, T. H., Fountain, A. G., and Doran, P. T.: Climatology of katabatic winds in the McMurdo dry valleys, southern Victoria Land, Antarctica, J. Geophys. Res. Atmos., 109, https://doi.org/10.1029/2003jd003937, 2004.

https://doi.org/10.5194/egusphere-2023-2515
Preprint. Discussion started: 15 December 2023

Östin, R. and Andersson, S.: Frost growth parameters in a forced air stream, Int. J. Heat Mass Transf., 34, 1009–1017, https://doi.org/10.1016/0017-9310(91)90012-4, 1991.

Philippe, M., Tison, J.-L., Fjøsne, K., Hubbard, B., Kjær, H. A., Lenaerts, J., Drews, R., Sheldon, S. G., De Bondt, K., and Claeys, P.: Ice core evidence for a 20th century increase in surface mass balance in coastal Dronning Maud Land, East Antarctica, Cryosph., 10, 2501–2516, 2016.

Pohjola, V., Moore, J., Isaksson, E., Jauhiainen, T., Martma, T., Meijer, H. A. J., Vaikmäe, R., and Van de Wal, R. S. W.: An ice core record from Lomonsovfonna, Svalbard: investigation of depositional signals with respect to melt, J. Geophys. Res., 10, 2002.

Pratap, B., Dey, R., Matsuoka, K., Moholdt, G., Lindbäck, K., Goel, V., Laluraj, C. M., and Thamban, M.: Three-decade spatial patterns in surface mass balance of the Nivlisen Ice Shelf, central Dronning Maud Land, East Antarctica, J. Glaciol., 68, 174–186, https://doi.org/DOI: 10.1017/jog.2021.93, 2022.

Reboita, M. S., da Rocha, R. P., Ambrizzi, T., and Gouveia, C. D.: Trend and teleconnection patterns in the climatology of extratropical cyclones over the Southern Hemisphere, Clim. Dyn., 45, 1929–1944, https://doi.org/10.1007/s00382-014-2447-3, 2015.

Rotschky, G., Holmlund, P., Isaksson, E., Mulvaney, R., Oerter, H., Van Den Broeke, M. R., and Winther, J.-G.: A new surface accumulation map for western Dronning Maud Land, Antarctica, from interpolation of point measurements, J. Glaciol., 53, 385–398, 2007.

Rott, H., Skvarca, P., and Nagler, T.: Rapid Collapse of Northern Larsen Ice Shelf, Antarctica, Science (80-.)., 271, 788–792, https://doi.org/10.1126/SCIENCE.271.5250.788, 1996.

Sato, K. and Simmonds, I.: Antarctic skin temperature warming related to enhanced downward longwave radiation associated with increased atmospheric advection of moisture and temperature, Environ. Res. Lett., 16, 064059, https://doi.org/10.1088/1748-9326/AC0211, 2021.

Scambos, T. A., Hulbe, C., Fahnestock, M., and Bohlander, J.: The link between climate warming and break-up of ice shelves in the Antarctic Peninsula, J. Glaciol., 46, 516–530, https://doi.org/10.3189/172756500781833043, 2000.

Scambos, T. A., Bohlander, J. A., Shuman, C. A., and Skvarca, P.: Glacier acceleration and thinning after ice shelf collapse in the Larsen B embayment, Antarctica, Geophys. Res. Lett., 31, 18402, https://doi.org/10.1029/2004GL020670, 2004.

Schlosser, E. and Oerter, H.: Shallow firn cores from Neumayer, Ekströmisen, Antarctica: a comparison of accumulation rates and stable-isotope ratios, Ann. Glaciol., 35, 91–96, 2002.

Schlosser, E., Manning, K. W., Powers, J. G., Duda, M. G., Birnbaum, G., and Fujita, K.: Characteristics of high-

https://doi.org/10.5194/egusphere-2023-2515
Preprint. Discussion started: 15 December 2023

precipitation events in Dronning Maud Land, Antarctica, J. Geophys. Res. Atmos., 115, https://doi.org/10.1029/2009JD013410, 2010.

Silber, I., Verlinde, J., Wang, S. H., Bromwich, D. H., Fridlind, A. M., Cadeddu, M., Eloranta, E. W., and Flynn, C. J.: Cloud influence on ERA5 and AMPS surface downwelling longwave radiation biases in West Antarctica, J. Clim., 32, 7935–7949, https://doi.org/10.1175/JCLI-D-19-0149.1, 2019.

Sinclair, M. R.: Record-high temperatures in the Antarctic—A synoptic case study, Mon. Weather Rev, 109, 2234–2242, 1981.

Sinclair, V. A. and Dacre, H. F.: Which Extratropical Cyclones Contribute Most to the Transport of Moisture in the Southern Hemisphere?, J. Geophys. Res. Atmos., 124, 2525–2545, https://doi.org/10.1029/2018JD028766, 2019.

Speirs, J. C., Steinhoff, D. F., McGowan, H. A., Bromwich, D. H., and Monaghan, A. J.: Foehn Winds in the McMurdo Dry Valleys, Antarctica: The Origin of Extreme Warming Events, J. Clim., 23, 3577–3598, https://doi.org/10.1175/2010JCLI3382.1, 2010.

Tetzner, D., Thomas, E., and Allen, C.: A validation of ERA5 reanalysis data in the southern antarctic peninsula—Ellsworth land region, and its implications for ice core studies, Geosci., 9, https://doi.org/10.3390/geosciences9070289, 2019.

Thiery, W., Gorodetskaya, I. V, Bintanja, R., Van Lipzig, N. P. M., Van den Broeke, M. R., Reijmer, C. H., and Kuipers Munneke, P.: Surface and snowdrift sublimation at Princess Elisabeth station, East Antarctica, Cryosph., 6, 841–857, 2012.

Turner, J., Colwell, S. R., Marshall, G. J., Lachlan-Cope, T. A., Carleton, A. M., Jones, P. D., Lagun, V., Reid, P. A., and Iagovkina, S.: The SCAR READER Project: Toward a High-Quality Database of Mean Antarctic Meteorological Observations, J. Clim., 17, 2890–2898, https://doi.org/https://doi.org/10.1175/1520-0442(2004)017<2890:TSRPTA>2.0.CO;2, 2004.

Turner, J., Lu, H., King, J. C., Carpentier, S., Lazzara, M., Phillips, T., and Wille, J.: An Extreme High Temperature Event in Coastal East Antarctica Associated With an Atmospheric River and Record Summer Downslope Winds, Geophys. Res. Lett., 49, 1–11, https://doi.org/10.1029/2021GL097108, 2022.

Vaughan, D. G., Bamber, J. L., Giovinetto, M., Russell, J., and Cooper, A. P. R.: Reassessment of net surface mass balance in Antarctica, J. Clim., 12, 933–946, 1999.

Vihma, T., Tuovinen, E., and Savijärvi, H.: Interaction of katabatic winds and near-surface temperatures in the Antarctic, J. Geophys. Res. Atmos., 116, 2011.

van Wessem, J. M., van de Berg, W. J., Noël, B. P. Y., van Meijgaard, E., Amory, C., Birnbaum, G., Jakobs, C. L.,

https://doi.org/10.5194/egusphere-2023-2515
Preprint. Discussion started: 15 December 2023

Krüger, K., Lenaerts, J. T. M., Lhermitte, S., Ligtenberg, S. R. M., Medley, B., Reijmer, C. H., van Tricht, K., Trusel, L. D., van Ulft, L. H., Wouters, B., Wuite, J., and van den Broeke, M. R.: Modelling the climate and surface mass balance of polar ice sheets using RACMO2 -- Part 2: Antarctica (1979--2016), Cryosph., 12, 1479–1498, https://doi.org/10.5194/tc-12-1479-2018, 2018.

van Wessem, J. M., van de Berg, W. J., and van den Broeke, M. R.: Data set: Monthly averaged RACMO2.3p2 variables; Antarctica, https://doi.org/10.5281/zenodo.7760491, March 2023.

Wille, J. D., Favier, V., Dufour, A., Gorodetskaya, I. V., Turner, J., Agosta, C., and Codron, F.: West Antarctic surface melt triggered by atmospheric rivers, Nat. Geosci., 12, 911–916, https://doi.org/10.1038/s41561-019-0460-1, 2019.

Zhu, J., Xie, A., Qin, X., Wang, Y., Xu, B., and Wang, Y.: An assessment of ERA5 reanalysis for antarctic near-surface air temperature, Atmosphere (Basel)., 12, https://doi.org/10.3390/atmos12020217, 2021.

Zou, X., Bromwich, D. H., Montenegro, A., Wang, S. H., and Bai, L.: Major surface melting over the Ross Ice Shelf part I: Foehn effect, Q. J. R. Meteorol. Soc., 147, 2874–2894, https://doi.org/10.1002/QJ.4104, 2021a.

Zou, X., Bromwich, D. H., Montenegro, A., Wang, S. H., and Bai, L.: Major surface melting over the Ross Ice Shelf part II: Surface energy balance, Q. J. R. Meteorol. Soc., 147, 2895–2916, https://doi.org/10.1002/QJ.4105, 2021b.